Accepted Manuscript

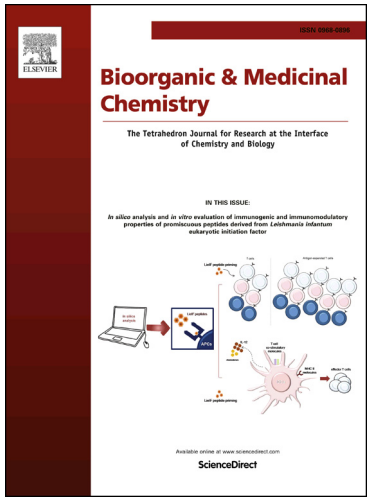

Synthesis, Structure-Activity Relationships, and Mechanistic Studies of 5-Arylazo-tropolone Derivatives as Novel Xanthine Oxidase (XO) Inhibitors

Daisuke Sato, Takuya Kisen, Mina Kumagai, Kiminori Ohta

PII: S0968-0896(17)32132-6
DOI: https://doi.org/10.1016/j.bmc.2017.12.017
Reference: BMC 14122

To appear in: *Bioorganic & Medicinal Chemistry*

Received Date: 2 November 2017
Revised Date: 8 December 2017
Accepted Date: 10 December 2017

Please cite this article as: Sato, D., Kisen, T., Kumagai, M., Ohta, K., Synthesis, Structure-Activity Relationships, and Mechanistic Studies of 5-Arylazo-tropolone Derivatives as Novel Xanthine Oxidase (XO) Inhibitors, *Bioorganic & Medicinal Chemistry* (2017), doi: https://doi.org/10.1016/j.bmc.2017.12.017

Graphical Abstract

To create your abstract, type over the instructions in the template box below.
Fonts or abstract dimensions should not be changed or altered.

Synthesis, Structure-Activity Relationships, and Mechanistic Studies of 5-Arylazotropolone Derivatives as Novel Xanthine Oxidase (XO) Inhibitors

Leave this area blank for abstract info.

Daisuke Sato, Takuya Kisen, Mina Kumagai, Kiminori Ohta*

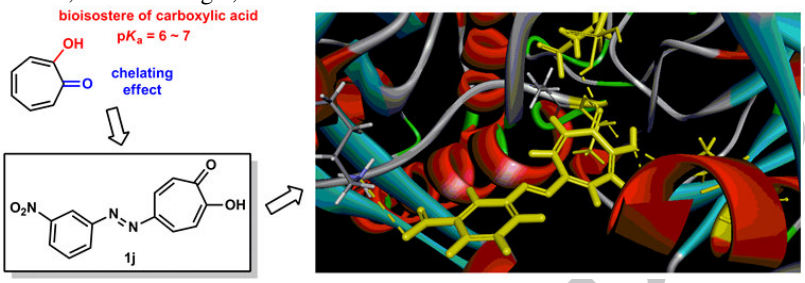

Bioorganic & Medicinal Chemistry
journal homepage: www.elsevier.com

Synthesis, Structure-Activity Relationships, and Mechanistic Studies of 5-Arylazotropolone Derivatives as Novel Xanthine Oxidase (XO) Inhibitors

Daisuke Sato, Takuya Kisen, Mina Kumagai, Kiminori Ohta*

Faculty of Pharmaceutical Sciences, Tohoku Medical and Pharmaceutical University, 4-4-1 Komatsushima, Aoba-ku, Sendai 981-8558, Japan

ARTICLE INFO

Article history:
Received
Received in revised form
Accepted
Available online

Keywords:
xanthine oxidase
enzyme inhibitor
tropolone
kinetic study
docking-simulation study

ABSTRACT

Xanthine oxidase (XO) is an enzyme that contains molybdenum at the active site and catalyzes the oxidation of purine bases to uric acid. Even though XO inhibitors are widely used for the treatment of hyperuricemia and gout, only very few such compounds are clinically used as drugs for the treatment of these diseases. Given the unique physicochemical properties of tropolone, i.e., its chelating effect and the pKa value that is similar to that of carboxylic acid, we have synthesized 22 5-arylazotropolone derivatives as potential XO inhibitors. In vitro enzyme-inhibitory assays for XO revealed that 3-nitro derivative 1j showed the most potent XO inhibitory activity, which is by one order of magnitude more potent than allopurinol. An enzyme-kinetic study revealed that 1j inhibited the production of uric acid by XO both competitively and non-competitively. A docking-simulation study of 1j with XO suggested that the carbonyl and hydroxyl groups of the tropolone ring interact with the hydroxy group that acts as a ligand for molybdenum and the amino acid residues around the active site of XO.

1. Introduction

Xanthine oxidase (XO) is an enzyme that contains a molybdenum atom at the active site and catalyzes the oxidation of purine bases to uric acid.[1] Since a high level of uric acid in the blood is associated with gout, XO inhibitors are widely used for the treatment of hyperuricemia, and consequently gout.[2] Even though allopurinol was developed as an XO inhibitor over 60 years ago, it remains the most widely prescribed therapeutic drug for hyperuricemia and gout worldwide (Figure 1).[3] However, allopurinol and its metabolites may cause serious adverse effects on account of the purine skeleton.[4,5] On the other hand, febuxostat, which is a recently developed XO inhibitor, exhibits a non-purine skeleton and does not show the side effects observed for allopurinol (Figure 1).[6] Allopurinol and its active metabolite oxyprinol coordinate to the molybdenum atom at the active site of XO and inhibit the oxidation of hypoxanthine and xanthine to uric acid.[7,8] In contrast, febuxostat does not form coordination bonds with the molybdenum atom, but binds to the narrow aisle through which xanthine passes.[9,10] Its carboxylic acid group forms hydrogen bonds with the amino acid residues at the active site of XO. Although various XO inhibitors have been developed since allopurinol has been used as a therapeutic agent for gout, there are only a few clinically used XO inhibitors for the treatment of hyperuricemia and gout.[11] Therefore, the development of novel XO inhibitors with non-purine skeletons should be highly desirable, as they should increase treatment options for these diseases.

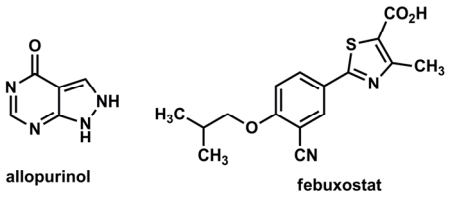

Figure 1. Chemical structures of allopurinol and febuxostat.

Tropolone is a seven-membered non-benzenoid aromatic compound that contains three double bonds conjugated with a carbonyl group and a hydroxyl group (Figure 2).[12] β-Thujaplicin is a tropolone-containing natural product that shows inhibitory activity against several enzymes.[13-16] We have previously reported that tropolone can act as a bioisostere of benzoic acid in the development of retinoic-acid-receptor modulators.[17] Several papers have already been published that use tropolone derivatives as ligands for metal complexes.[18-20] We thus considered that tropolone might bind to the molybdenum atom at the active site of XO in a chelating fashion similar to allopurinol, or attach to the narrow aisle to the molybdenum atom via the formation of hydrogen bonds similar to febuxostat. Based on the chemical structures of clinical XO inhibitors, and the synthetic advantages of tropolone derivatives, 5-arylazotropolone derivatives **1** and **2** were designed as novel XO inhibitors (Figure 2).

Herein, we describe the synthesis of 5-arylazotropolone derivatives **1** and **2**, as well as their structure-activity relationship

regarding the inhibition of XO. Additionally, we describe enzyme-kinetic and docking-simulation studies involving **1j**, which exhibited the most potent XO-inhibitory activity.

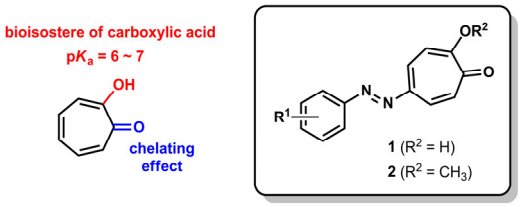

Figure 2. Structures of tropolone and the designed molecules (**1** and **2**) as novel XO inhibitors.

2. Results and discussion

*2.1. Synthesis of the tropolone derivatives **1** and **2***

Tropolone was synthesized from dicyclopentadiene **3** according to a previously reported procedure (Scheme 1).[21] Briefly, cyclopentadiene **4**, which was obtained from the cracking of **3** at 200 °C, was reacted with dichloroketene, which was obtained from the in-situ reaction of dichloroacetyl chloride with triethylamine, to give 7,7-dichlorobicyclo[3.2.0]hept-2-en-6-one (**5**) in 79% yield. Bicyclic intermediate **5** was subsequently treated with sodium acetate to give crude tropolone **6** in 95% yield. Vacuum distillation and recrystallization from AcOEt afforded pure **6** as colorless needles.

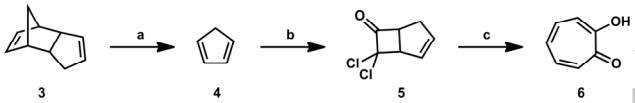

Scheme 1. Synthesis of tropolone. *Reagents and conditions:* a) 200 °C; b) $Cl_2CHCOCl$, Et_3N, pentane, 79%; c) NaOH, acetic acid, 95%.

Commercially available anilines (**7**) were transformed into the corresponding diazonium salts using sodium nitrite, and subsequently reacted with sodium troponate under basic conditions to give the corresponding 5-arylazotropolone derivatives (Scheme 2). Compound **1t** was treated with trimethylsilyldiazomethane to afford **2**, which contains a methoxy instead of a hydroxy group on the tropolone ring (Scheme 2).[22] All synthesized derivatives were purified by recrystallization due to the strong adsorption of tropolone derivatives on silica gel.

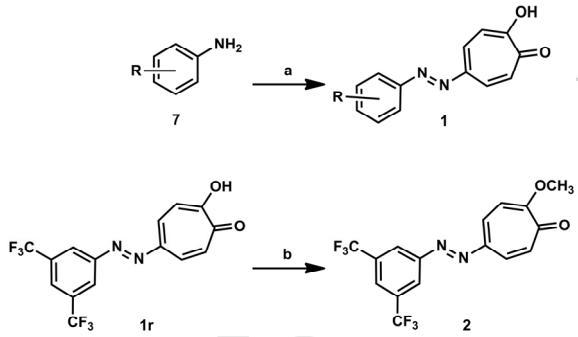

Scheme 2. Synthesis of tropolone derivatives **1** and **2**. *Reagents and conditions*: a) (i) 10% HCl aq., (ii) $NaNO_2$, (iii) sodium troponate, 10% NaOH aq., (iv) recrystallization, 2–62%; b) TMS diazomethane, MeOH, recrystallization, 31%.

*2.2. Biological evaluations of the synthesized compounds **1** and **2***

The XO-inhibitory activity of the synthesized compounds was evaluated by means of in vitro enzyme-inhibitory assays using XO from bovine milk and xanthine as a substrate.[23,24] XO-inhibitory rates (%) of each test compound at specific concentrations (100 μM – 10 nM) were determined based upon the quantity of uric acid, which is a metabolite of xanthine, estimated from the absorbance at 290 nm. IC_{50} values of the test compounds were calculated from the dose-response curves obtained from the XO-inhibitory rates at each concentration. The XO-inhibitory activity values of the test compounds are summarized in Table 1.

Table 1. IC_{50} values of tropolone derivatives **1** and **2** against XO.[a]

Compound	Ar	IC_{50}(μM)[b]	Compound	Ar	IC_{50} (μM)[b]	Compound	Ar	IC_{50} (μM)[b]
1a		45	**1i**	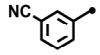	1.1	**1q**	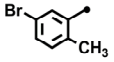	inactive
1b		8.9	**1j**	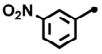	0.46	**1r**	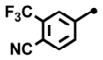	18
1c		17	**1k**	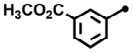	80	**1s**	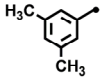	inactive
1d		inactive	**1l**		inactive	**1t**	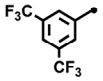	3.0
1e		inactive	**1m**	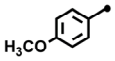	inactive	**1u**	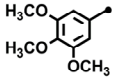	57
1f	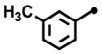	inactive	**1n**	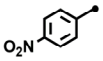	inactive	**2**		inactive
1g	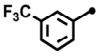	7.4	**1o**	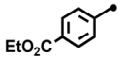	inactive	allopurinol		2.6
1h	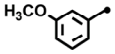	45	**1p**	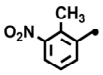	23			

[a]All XO inhibitory assays were treated with the test compounds (1 nM – 100 μM) in the presence of XO and xanthine as a substrate and performed in triplicate (n = 3). [b]IC_{50} values of the tested compounds were calculated from dose-response curves based on the inhibitory rate against XO.

Non-substituted derivative **1a** showed a ~ 20 times weaker XO-inhibitory activity than allopurinol. The introduction of fluorine and chlorine atoms at the meta position on the benzene ring increased the XO-inhibitory activity, while both *m*-bromo (**1d**) and *m*-iodo derivatives (**1e**) were inactive. Although m-methyl derivative **1f** was inactive, trifluoromethyl derivative **1g** inhibited the catalytic activity of XO (IC_{50} = 7.4 μM). It seems that the presence of an electron-withdrawing group at the meta position of the benzene ring plays an important role for the inhibitory activity of XO. Given the Hammett constant of the methoxy group at the meta position (σ_m = 0.12), **1h** should be active for the inhibition of XO.[25] However, the size of the methoxy group might be slightly large for the ligand-binding pocket of XO. While both **1i** and **1j**, which contain strong electron-withdrawing groups, showed more potent XO-inhibitory activity than allopurinol, **1j** acted as the most potent inhibitor among all tested compounds. Even though ester groups are also electron withdrawing, the XO-inhibitory activity of **1k** was a very weak. This low activity may be attributed to the relatively large size of the ester group relative to the ligand-binding pocket of XO.

Interestingly, **1l**–**1o**, which contain electron-withdrawing groups at the para position of the benzene ring, did not show any inhibitory activity, even though **1n** contains a nitro group with highly electron-withdrawing properties. The observed activity patterns may be rationalized in terms of a steric repulsion between the substituents at the para position of the benzene ring and the amino-acid residues on the ligand-binding pocket of XO.

Compound **1p**, which contains an additional methyl group at the ortho position of **1j**, showed weak XO-inhibitory activity and an IC_{50} value of 23 μM, which is ~ 50 times lower than that of the parent compound (**1j**). Compound **1q**, which contains a methyl group at the ortho position relative to **1d**, was also inactive. Probably, the presence of a methyl group at the ortho position negatively affect the XO-inhibitory activity via the electron-donating nature or some sterically hinderance. The XO-inhibitory activity of **1r** decreased remarkably compared to that of the parent compound (**1g**) due to the introduction of a cyano group at the para position. As shown for **1f** and **1g,** similar substituent effects for the XO-inhibitory activity by methyl and trifluoromethyl groups were also observed in 3,5-dimethylphenyl derivative **1s** and 3,5-bis(trifluoromethyl)phenyl derivative **1t**, respectively. Although **1s** was inactive, the XO inhibitory activity of **1t** was more potent than that of the parent compound (**1g**) and similar to that of allopurinol. This might be caused by the electronic substituent effects arising from the presence of two trifluoromethyl groups at the meta position of **1t**. Trimethoxy derivative **1u** maintained weak XO-inhibitory activity owing to the presence of two methoxy groups at the meta position, albeit that there are three methoxy groups present on the benzene ring. When the hydroxy group of the tropolone ring of **1t** was protected with a methyl group, the XO-inhibitory activity of **1t**, which is similar to that of allopurinol, ceased (compound **2**). Accordingly, we concluded that the hydroxy group of the tropolone ring should interact with the active site of XO, and that the enhancement of the acidity of the hydroxy group relates closely to the increase of the XO-inhibitory activity.

*2.3. Kinetic studies on **1j** for XO-inhibitory process*

To determine the XO-inhibitory mechanisms of 5-arylazotropolone derivatives, we carried out kinetic studies on

the selected compound **1j**.[23,24] A Lineweaver-Burk (LB) plot analysis on the oxidation of xanthine by XO in the presence (0.25, 0.5, or 1.0 μM) or absence of **1j** was performed (Figure 3). K_m and V_{max} values for each concentration of **1j** were estimated from the intersections of the x- and y-axes on the LB plot, respectively (Table 2). The K_m values increased with increasing concentrations of **1j**, while the V_{max} values exhibited a concentration-dependent decrease. Thus, an intersection of straight lines obtained from each concentration is located between the x- and y-axes plots, suggesting that **1j** engages in competitive and non-competitive XO-inhibitory mechanisms, in a fashion similar to allopurinol and febuxostat.[8,9]

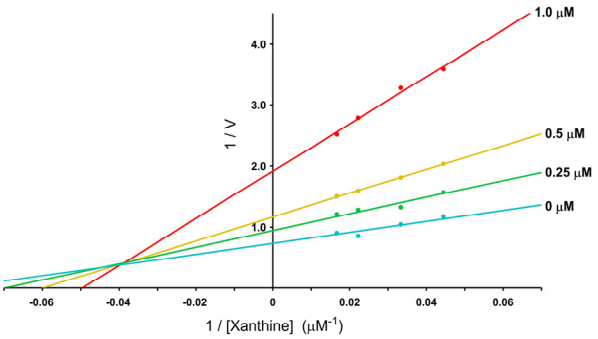

Figure 3. Lineweaver-Burk plots for the oxidation of xanthine by XO in the presence and absence of **1j**.

Table 2. K_m and V_{max} values for XO in the presence and absence of **1j**.[a]

1j (μM)	K_m (μM)	V_{max} (nmol / min)
0	12.08	1.35
0.25	14.35	1.06
0.5	16.70	0.86
1.0	20.14	0.52

[a] K_m and V_{max} values were estimated from enzyme-kinetic studies.

2.4. Docking simulation study of 1j using XO

A docking-simulation study of XO (PDB: 1N5X) with the selected inhibitor **1j** was carried out using an automatic docking program (Discovery Studio 4.5/CDOCKER).[26] The docking mode of **1j** at the active site of XO is shown in Figure 4. The carbonyl group of the tropolone ring engaged in hydrogen bonds with a hydroxy group bound to the molybdenum ion at the active site and the NH group of Ala1079 as the backbone. The acidic hydroxy group of the tropolone ring interacted with the guanidine group of Arg880 of XO. These results suggest that the loss of the XO-inhibitory activity of **2** is due to the protection of the hydroxy group by the methyl group. Furthermore, the potent inhibitory activity observed in the tropolone derivatives with an electron-withdrawing group might be caused by the interaction between the troponate anion derived from the acidic hydroxy group and the cationic guanidinium group of Arg880. It seems that a nitro group on the benzene ring of **1j** interacted with the amino acid residue of Lys771. The poor inhibitory activity of the ester group in **1k** could be explained by the steric repulsion with the amino acid residue of Lys771. Several hydrophobic amino-acid residues of XO are close to the tropolone and benzene rings on account of the hydrophobic interactions, as shown in the X-ray diffraction co-crystal structure of febuxostat with XO.[9,10]

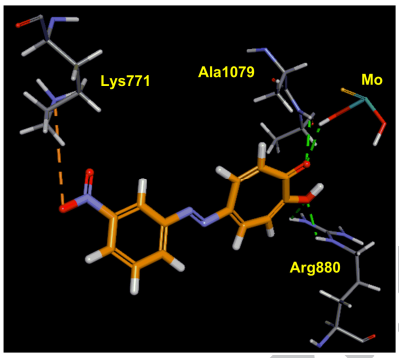

Figure 4. Plausible binding mode of **1j** with XO obtained from a docking-simulation study.

3. Conclusion

Based on the chemical properties of tropolone, i.e., the chelating effect and the pK_a value that is similar to that of carboxylic acid, simple and facile azotropolone derivatives were designed and synthesized as novel XO inhibitors. The hydroxy and carbonyl groups of the tropolone ring of the azotropolone derivatives are very important for the XO-inhibitory activity. Compound **1j** showed a potent XO-inhibitory activity that was ca. tenfold higher than that of allopurinol, and acted as a mixed-type inhibitor with both competitive and non-competitive inhibition mechanisms, similar to those of allopurinol and febuxostat. Docking-simulation studies of **1j** with XO suggested three important interactions: (i) hydrogen bonds between the carbonyl group of the tropolone ring, a hydroxy group bound to the molybdenum ion, and the NH group of Ala1079 as a backbone; (ii) a hydrogen bond between the acidic hydroxy group of the tropolone ring and the guanidine group of Arg880, and (iii) an electrostatic interaction between the nitro group on the benzene ring and the amino acid residue of Lys771. SAR studies of a linking group and tropolone ring of **1j**, as well as QSAR studies on the pK_a values of the azotropolone derivatives are currently in progress in our laboratory in order to discover more potent and non-toxic XO inhibitors.

4. Experimental

4.1. General Considerations

Melting points were determined using a Yanaco micro melting point apparatus and are uncorrected. ^{1}H NMR and ^{13}C NMR spectra were recorded on JEOL JNM-EX-270 and JNM-LA-400 spectrometers. Chemical shifts for the ^{1}H NMR spectra are referenced to tetramethylsilane (0.0 ppm) as an internal standard. Chemical shifts for the ^{13}C NMR spectra are referenced to the signals of residual non-deuterated solvents within the deuterated solvents. The splitting patterns are assigned as follows: s (singlet), d (doublet), t (triplet), q (quartet), and m (multiplet). Mass spectra were recorded on a JEOL JMS-DX-303 spectrometer. Elemental analyses were performed on a Perkin Elmer 2400 CHN spectrometer. TLC was performed on F254 silica gel from Merck. Reagents were purchased from Wako Pure Chemical Industries, Ltd., Sigma-Aldrich Co., and Tokyo Chemical Industry, Ltd. (TCI). All solvents (reagent quality) were purchased from common commercial sources and used

without further purification. Yields of the tested compounds in this section represent those after recrystallization.

*4.1.1. (E)-5-phenyl-2-hydroxycyclohepta-2,4,6-trienone (**1a**)*

A solution of aniline **7a** (188 mg, 2.0 mmol) in 6 mL of 10% hydrochloric acid was treated dropwise with a 2 N aqueous solution of $NaNO_2$ (2 mL, 4.0 mmol) at 0 °C, and the mixture was stirred at 0 °C for 30 min to prepare the corresponding diazonium salt *in situ*. A solution of sodium troponate, which was prepared from tropolone (262 mg, 2.2 mmol) and 10 mL of a 10% aqueous solution of NaOH, was added at 0 °C, and the reaction mixture was stirred at room temperature overnight. The mixture was poured into 10% hydrochloric acid, and the thus obtained brown precipitate was collected, washed with water, and dried to afford 571 mg (quantitative yield) of crude **1a**, which was purified by recrystallization from AcOEt to afford 116 mg (25% yield) of brown needles; mp 159–160 °C; ^{1}H NMR (400 MHz, DMSO-d_6) δ (ppm) 7.36 (d, J = 12.0 Hz, 2H), 7.39–7.62 (m, 3H), 7.87 (dd, J = 2.0 Hz, 8.4 Hz, 2H), 8.11 (dd, J = 1.2 Hz, 12.0 Hz, 2H); ^{13}C NMR (100 MHz, DMSO-d_6) δ (ppm) 122.6, 123.9, 129.5, 131.6, 133.0, 149.6, 151.6, 171.9; IR (KBr, cm^{-1}) 3172 (OH), 1612 (C=O), 1560 (N=N); MS (EI) *m/z* 77 (100%), 226 (M^+); HRMS Calcd. for $C_{13}H_{10}N_2O_2$: 226.0742, Found: 226.0736; Anal. Calcd. for $C_{13}H_{10}N_2O_2$ 0.1 H_2O: C 68.47, H 4.51, N 12.29, Found: C 68.42, H 4.50, N 12.19.

*4.1.2. (E)-5-(3-Fluorophenyl)-2-hydroxycyclohepta-2,4,6-trienone (**1b**)*

Compound **1b** was prepared by the same method as described for the synthesis of **1a** using 3-fluoroaniline (222 mg, 2.0 mmol) instead of aniline; 182 mg (34% yield); red needles (AcOEt); mp 177–178 °C; ^{1}H NMR (400 MHz, DMSO-d_6) δ (ppm) 7.35 (dd, J = 1.9 Hz, 12.2 Hz, 2H), 7.44 (ddd, J = 1.1 Hz, 2.7 Hz, 8.4 Hz, 1H), 7.59–7.67 (m, 2H), 7.77 (ddd, J = 1.1 Hz, 2.7 Hz, 8.1 Hz, 1H), 8.11 (dd, J = 1.1 Hz, 11.9 Hz, 2H); ^{13}C NMR (100 MHz, DMSO-d_6) δ (ppm) 107.5, 107.7, 118.0, 118.2, 120.5, 123.8, 131.3, 133.3, 161.5, 163.9, 172.2; MS (EI) *m/z* 244 (M^+, 100%); HRMS Calcd. for $C_{13}H_9FN_2O_2$: 244.0648, Found: 244.0642; Anal. Calcd. for $C_{13}H_9FN_2O_2$: C 63.93, H 3.71, N 11.47, Found: C 63.91 H 3.79, N 11.43.

*4.1.3. (E)-5-(3-Chlorophenyl)-2-hydroxycyclohepta-2,4,6-trienone (**1c**)*

Compound **1c** was prepared by the same method as described for the synthesis of **1a** using 3-chloroaniline (290 mg, 2.3 mmol) instead of aniline; 245 mg (47% yield); red/brown needles (AcOEt); mp 170–172 °C; ^{1}H NMR (400 MHz, DMSO-d_6) δ (ppm) 7.34 (d, J = 12.0 Hz, 2H), 7.62-7.63 (m, 2H), 7.84–7.87 (m, 2H), 8.11 (dd, J = 1.2 Hz, 12.0 Hz, 2H); ^{13}C NMR (100 MHz, DMSO-d_6) δ (ppm) 120.9, 122.6, 123.8, 130.9, 131.3, 133.4, 134.2, 149.4, 152.5, 172.3; MS (EI) *m/z* 111 (100%), 260 (M^+); HRMS Cacld. for $C_{13}H_9{}^{35}ClN_2O_2$: 260.0353, Found: 260.0347, Cacld. for $C_{13}H_9{}^{37}ClN_2O_2$: 262.0323, Found: 262.0331; Anal. Calcd. for $C_{13}H_9ClN_2O_2$ 0.1 H_2O: C 59.48, H 3.53, N 10.68, Found: C 59.40, H 3.49, N 10.62.

*4.1.4. (E)-5-(3-Bromophenyl)-2-hydroxycyclohepta-2,4,6-trienone (**1d**)*

Compound **1d** was prepared by the same method as described for the synthesis of **1a** using 3-bromoaniline (390 mg, 2.3 mmol) instead of aniline; 249 mg (35% yield); brown needles (AcOEt); mp 170–171 °C; ^{1}H NMR (400 MHz, DMSO-d_6) δ (ppm) 7.36 (d, J = 12.0 Hz, 2H), 7.56 (t, J = 8.0 Hz, 1H), 7.75 (dd, J = 0.8 Hz, 8.0 Hz, 1H), 7.90 (dd, J = 0.8 Hz, 8.0 Hz, 1H), 7.97 (t, J = 2Hz, 1H), 8.12 (d, J = 12.4 Hz, 2H); ^{13}C NMR (100 MHz, DMSO-d_6) δ (ppm) 122.6, 123.2, 123.6, 123.8, 131.6, 133.4, 133.8, 149.4, 152.6, 172.1; MS (EI) *m/z* 304 (M^+, 100%); HRMS Calcd. for $C_{13}H_9{}^{79}BrN_2O_2$: 303.9847, Found: 303.9854, HRMS Calcd. for $C_{13}H_9{}^{81}BrN_2O_2$: 305.9827, Found: 305.9830; Anal. Calcd. for $C_{13}H_9BrN_2O_2$: C 51.17, H 2.97, N 9.18, Found: C 50.87, H 3.00, N 9.17.

*4.1.5. (E)-5-(3-Iodophenyl)-2-hydroxycyclohepta-2,4,6-trienone (**1e**)*

Compound **1e** was prepared by the same method as described for the synthesis of **1a** using 3-iodoaniline (456 mg, 2.1 mmol) instead of aniline; 149 mg (20% yield); purple/brown needles (AcOEt); mp 198–201 °C; ^{1}H NMR (400 MHz, DMSO-d_6) δ (ppm) 7.35 (d, J = 12.0 Hz, 2H), 7.40 (t, J = 8.0 Hz, 7.6 Hz 1H), 7.90 (dd, J = 1.2 Hz, 7.6 Hz, 2H), 8.11 (dd, J = 1.2 Hz, 12.4 Hz, 2H), 8.13 (dd, J = 1.6 Hz, 1H); ^{13}C NMR (100 MHz, DMSO-d_6) δ (ppm) 95.6, 123.6, 123.8, 129.4, 131.6, 133.3, 139.7, 149.4, 152.4, 172.1; MS (EI) *m/z* 352 (M+, 100%); HRMS Calcd. for $C_{13}H_9IN_2O_2$: 351.9709, Found: 351.9707; Anal. Calcd. for $C_{13}H_9IN_2O_2$: C 44.34, H 2.58, N 7.96, Found: C 44.09, H 2.68, N 7.82.

*4.1.6. (E)-5-(3-Tolyl)-2-hydroxycyclohepta-2,4,6-trienone (**1f**)*

Compound **1f** was prepared by the same method as described for the synthesis of **1a** using *m*-toluidine (260 mg, 2.4 mmol) instead of aniline; 65 mg (14% yield); brown thin needles (AcOEt); mp 170–171 °C; ^{1}H NMR (400 MHz, DMSO-d_6) δ (ppm) 2.41(s, 3H), 7.35 (dd, J = 1.2 Hz, 12.0 Hz, 2H), 7.40 (t, J = 7.6 Hz, 8.4 Hz 1H), 7.67 (dd, J = 1.2 Hz, 6.0 Hz, 2H), 8.10 (dd, J =1.2 Hz, 12.0 Hz, 2H); ^{13}C NMR (100 MHz, DMSO-d_6) δ (ppm) 20.9, 120.3, 122.6, 123.9, 129.3, 132.3, 132.9, 139.0, 149.6 151.6, 171.9; MS (EI) *m/z* 240 (M^+), 91 (100%); HRMS Calcd. for $C_{14}H_{12}N_2O_2$: 240.0899, Found: 240.0893; Anal. Calcd. for $C_{14}H_{12}N_2O_2$: C 69.99, H 5.03, N 11.66, Found: C 70.05, H 5.12, N 11.56.

*4.1.7. (E)-5-(3-Trifluoromethylphenyl)-2-hydroxycyclohepta-2,4,6-trienone (**1g**)*

Compound **1g** was prepared by the same method as described for the synthesis of **1a** using 3-(trifluoromethyl)aniline (328 mg, 2.0 mmol) instead of aniline; 157 mg (26% yield); red/purple needles (AcOEt); mp 189–192 °C; ^{1}H NMR (400 MHz, DMSO-d_6) δ (ppm) 7.36 (d, J = 12.2 Hz, 2H), 7.84 (t, J = 7.8 Hz, 1H), 7.92 (d, J = 7.6 Hz, 1H), 8.15 (dd, J = 7.0 Hz, 12.2 Hz, 4H); ^{13}C NMR (100 MHz, DMSO-d_6) δ (ppm) 118.4, 122.5, 123.8, 125.2, 126.9. 127.7, 130.3, 131.0, 133.5, 149.5, 151.6, 172.2; MS (EI) *m/z* 145 (100%), 294 (M^+); HRMS Calcd. for $C_{14}H_9FN_2O_2$: 294.0616, Found: 294.0624; Anal. Calcd. for $C_{14}H_9FN_2O_2$: C 57.15, H 3.08, N 9.52, Found: C 56.85, H 3.13, N 9.52.

*4.1.8. (E)-5-(3-Methoxyphenyl)-2-hydroxycyclohepta-2,4,6-trienone (**1h**)*

Compound **1h** was prepared by the same method as described for the synthesis of **1a** using *m*-anisidine (754 mg, 6.1 mmol) instead of aniline; 151 mg (10% yield); brown prisms (AcOEt); mp 155–157 °C; ^{1}H NMR (400 MHz, DMSO-d_6) δ (ppm) 3.84 (s, 3H), 7.12–7.16 (m, 1H), 7.36 (d, J = 12.4 Hz, 2H),

7.38–7.39 (m, 1H), 7.49 (s, 1H), 7.48–7.53 (m, 1H), 8.09 (d, J = 12.4 Hz, 2H); ^{13}C NMR (100 MHz, DMSO-d_6) δ (ppm) 55.4, 106.1, 116.3, 117.8, 123.8, 130.3, 133.0, 149.5, 152.8, 160.1, 171.9; MS (EI) m/z 107 (100%), 256 (M^+); HRMS Calcd. for $C_{14}H_{12}N_2O_3$: 256.0849, Found 256.0846, Anal. Calcd. for $C_{14}H_{12}N_2O_3$: C 65.61, H 4.72, N 10.93 Found: C 65.36, H 4.71, N 10.93

*4.1.9. (E)-5-(3-Cyanophenyl)-2-hydroxycyclohepta-2,4,6-trienone (**1i**)*

Compound **1i** was prepared by the same method as described for the synthesis of **1a** using 3-aminobenzonitrile (236 mg, 2.0 mmol) instead of aniline; 63 mg (13% yield); red needles (AcOEt); mp 199–201 °C; ^{1}H NMR (400 MHz, DMSO-d_6) δ (ppm) 7.36 (d, J = 12.2 Hz, 2H), 7.79 (t, J = 8.0 Hz, 1H), 8.01 (d, J = 7.6 Hz, 1H), 8.12 (d, J = 12.0 Hz, 2H), 8.16 (d, J = 1.9 Hz, 1H), 8.26 (t, J = 1.7 Hz, 1H), ^{13}C NMR (100 MHz, DMSO-d_6) δ (ppm) 112.6, 118.1, 123.8, 126.0, 127.1, 131.0, 133.5, 134.5, 149.3, 151.5, 172.4; MS (EI) m/z 251 (M^+, 100%); HRMS Calcd. for $C_{14}H_9N_3O_2$: 251.0695, Found: 251.0691; Anal. Calcd. for $C_{14}H_9N_3O_2$: C 66.93, H 3.61, N 16.73, Found: C 66.63, H 3.68, N 16.64.

*4.1.10. (E)-5-(3-Nitrophenyl)-2-hydroxycyclohepta-2,4,6-trienone (**1j**)*

Compound **1j** was prepared by the same method as described for the synthesis of **1a** using 3-nitroaniline (277 mg, 2.0 mmol) instead of aniline; 301 mg (55% yield); red/brown needles (AcOEt); mp 231–232 °C; ^{1}H NMR (400 MHz, DMSO-d_6) δ (ppm) 7.35 (d, J = 11.6 Hz, 2H), 7.89 (t, J = 8.0 Hz, 1H), 8.15 (d, J = 11.6 Hz, 2H), 8.31 (d, J = 7.6 Hz, 1H), 8.39 (d, J = 7.2 Hz, 1H), 8.52 (s, 1H); ^{13}C NMR (100 MHz, DMSO-d_6) δ (ppm) 115.5, 123.7, 125.2, 129.6, 131.1, 133.6, 148.7, 151.8, 152.4, 172.4; MS (EI) m/z 271 (M^+, 100%); HRMS Calcd. for $C_{13}H_9N_3O_4$: 271.0594, Found: 271.0597; Anal. Calcd. for $C_{13}H_9N_3O_4 \cdot 0.1\ H_2O$: C 57.18, H 3.40, N 15.39, Found: C 57.10, H 3.24, N 15.78.

*4.1.11. (E)-5-(3-Methoxycarbonylphenyl)-2-hydroxycyclohepta-2,4,6-trienone (**1k**)*

Compound **1k** was prepared by the same method as described for the synthesis of **1a** using methyl 3-aminobanzoate (604 mg, 4.0 mmol) instead of aniline; 203 mg (36% yield): brown thin needles (AcOEt); mp 202–206 °C; ^{1}H NMR (400 MHz, DMSO-d_6) δ (ppm) 3.88 (s, 3H), 7.36 (d, J = 12.0 Hz, 2H), 7.74 (t, J = 7.8 Hz, 1H), 8.11–8.15 (m, 4H), 8.33 (d, J = 1.7 Hz, 1H), ^{13}C NMR (100 MHz, DMSO-d_6) δ (ppm) 52.5, 122.5, 123.8, 127.8, 130.3, 131.0, 131.6, 133.3, 149.5, 151.5, 165.6, 172.1; MS (EI) m/z 135 (100%), 284 (M^+); HRMS Calcd. for $C_{15}H_{12}N_2O_4$: 284.0797, Found: 284.0798; Anal. Calcd. for $C_{15}H_{12}N_2O_4$: C 63.38, H 4.25, N 9.85, Found: C 62.75, H 4.24, N 9.73.

*4.1.12. (E)-5-(4-Fluorophenyl)-2-hydroxycyclohepta-2,4,6-trienone (**1l**)*

Compound **1l** was prepared by the same method as described for the synthesis of **1a** using 4-fluoroaniline (243 mg, 2.2 mmol) instead of aniline; 152 mg (33% yield); yellow/brown plates (AcOEt); mp 201–202 °C; ^{1}H NMR (400 MHz, DMSO-d_6) δ (ppm) 7.36 (d, J = 12.0 Hz, 2H), 7.43 (t, J = 8.8 Hz, 2H), 7.94 (dt, J = 5.4 Hz, 9.0 Hz, 2H), 8.08 (d, J = 12.0 Hz, 2H); ^{13}C NMR (100 MHz, DMSO-d_6) δ (ppm) 116.4, 116.7, 123.9, 124.9, 125.0, 133.0, 148.4, 149.6, 162.6, 165.1, 171.9; MS (EI) m/z 95 (100%), 244 (M^+); HRMS Calcd. for $C_{13}H_9FN_2O_2$: 244.0648, Found: 244.0655; Anal. Calcd. for $C_{13}H_9FN_2O_2 \cdot 0.1\ H_2O$: C 63.46, H 3.77, N 11.39, Found: C 63.36, H 3.77, N 11.33.

*4.1.13. (E)-5-(4-Methoxyphenyl)-2-hydroxycyclohepta-2,4,6-trienone (**1m**)*

Compound **1m** was prepared by the same method as described for the synthesis of **1a** using p-anisidine (247 mg, 2.0 mmol) instead of aniline; 77 mg (15% yield); brown needles (AcOEt); mp 170–174 °C; ^{1}H NMR (400 MHz, DMSO-d_6) δ (ppm) 3.86 (s, 3H) 7.13 (d, J = 9.1 Hz, 2H), 7.35 (d, J = 12.2 Hz, 2H), 7.87 (d, J = 9.1 Hz, 2H), 8.05 (d, J = 12.0 Hz, 2H); ^{13}C NMR (100 MHz, DMSO-d_6) δ (ppm) 55.7, 114.7, 123.9, 124.7, 132.4, 145.9, 149.7, 162.1, 171.7; MS (EI) m/z 107 (100%), 256 (M^+); HRMS Calcd. for $C_{14}H_{12}N_2O_3$: 256.0848, Found: 256.0846; Anal. Calcd. for $C_{14}H_{12}N_2O_3$: C 65.62, H 4.72, N 10.93, Found: C 65.34, H 4.65, N 10.80.

*4.1.14. (E)-5-(4-Nitrophenyl)-2-hydroxycyclohepta-2,4,6-trienone (**1n**)*

Compound **1n** was prepared by the same method as described for the synthesis of **1a** using 4-nitroaniline (558 mg, 4.0 mmol) instead of aniline; 55 mg (10% yield); brown needles (AcOEt); mp 250–254 °C; ^{1}H NMR (270 MHz, DMSO-d_6) δ (ppm) 7.26 (d, J = 12.0 Hz, 2H), 8.01 (d, J = 9.1 Hz, 2H), 8.1 (d, J = 9.1 Hz, 2H), 8.41 (d, J = 12.0 Hz, 2H); ^{13}C NMR (100 MHz, DMSO-d_6) δ (ppm) 122.9, 123.8, 125.2, 133.8, 147.8, 154.5, 173.8; MS (EI) m/z 271 (M^+, 100%); HRMS Calcd. for $C_{13}H_9N_3O_4$: 271.0593, Found: 271.0596; Anal. Calcd. for $C_{13}H_9N_3O_4$: C 57.57, H 3.34, N 15.49, Found: C 57.46, H 3.35, N 15.23.

*4.1.15. (E)-5-(4-Ethoxycarbonylphenyl)-2-hydroxycyclohepta-2,4,6-trienone (**1o**)*

Compound **1o** was prepared by the same method as described for the synthesis of **1a** using ethyl 4-amionobenzoate (331 mg, 2.0 mmol) instead of aniline; 11 mg (2% yield); red needles (AcOEt); mp 208–210 °C; ^{1}H NMR (400 MHz, DMSO-d_6) δ (ppm) 1.34 (t, J = 7.1 Hz, 3H), 4.34 (q, J = 7.1 Hz, 2H), 7.33 (d, J = 11.9 Hz, 2H), 7.95 (d, J = 8.5 Hz, 2H), 8.12 (d, J = 12.0 Hz, 2H), 8.14 (d, J = 8.3 Hz, 2H); ^{13}C NMR (100 MHz, DMSO-d_6) δ (ppm) 14.1, 61.1, 122.6, 123.8, 130.5, 131.5, 133.5, 149.4, 153.9, 165.1, 172.5; MS (EI) m/z 149 (100%), 298 (M^+); HRMS Calcd. for $C_{16}H_{14}N_2O_4$: 298.0954, Found: 298.0958; Anal. Calcd. for $C_{16}H_{14}N_2O_4$: C 64.42, H 4.73, N 9.39, Found: C 64.35, H 4.72, N 9.28.

*4.1.16. (E)-5-(2-Methyl-3-nitrophenyl)diazenyl)-2-hydroxycyclohepta-2,4,6-trienone (**1p**)*

Compound **1p** was prepared by the same method as described for the synthesis of **1a** using 2-methyl-3-nitroaniline (312 mg, 2.1 mmol) instead of aniline; 34 mg (6% yield); brown prisms (AcOEt); mp 176–178 °C; ^{1}H NMR (400 MHz, DMSO-d_6) δ (ppm) 2.78 (s, 3H), 7.38 (d, J = 11.6 Hz, 2H), 7.58 (t, J = 7.6 Hz, 8.4 Hz, 1H), 7.84 (d, J = 8.0 Hz, 1H), 8.08 (d, J = 8.4 Hz, 1H), 8.15 (d, J = 12.0 Hz, 2H); ^{13}C NMR (100 MHz, DMSO-d_6) δ (ppm) 12.7, 119.9, 123.8, 126.3, 127.5, 131.3, 133.7, 149.9, 150.5, 151.1, 172.2; MS (EI) m/z 121 (100%), 285 (M^+); HRMS Calcd. for $C_{14}H_{11}N_3O_4$: 285.0750, Found: 285.0754; Anal. Calcd. for $C_{14}H_{11}N_3O_4 \cdot 0.1\ H_2O$: C 58.57, H 3.93, N 14.64, Found: C 58.18, H 3.81, N 14.51.

*4.1.17. (E)-5-(2-Methyl-5-bromophenyl)-2-hydroxycyclohepta-2,4,6-trienone (**1q**)*

Compound **1q** was prepared by the same method as described for the synthesis of **1a** using 5-bromo-2-methylaniline (373 mg, 2.0 mmol) instead of aniline; 49 mg (8%); brown needles (AcOEt); mp 162–164 °C; ^{1}H NMR (400 MHz, DMSO-d_6) δ (ppm) 2.62 (s, 3H), 7.36 (d, J = 12.1 Hz, 2H), 7.41 (d, J = 8.2 Hz, 1H), 7.61 (dd, J = 1.9 Hz, 8.2 Hz, 1H), 7.68 (d, J = 2.4 Hz, 1H), 8.13 (d, J = 12.1 Hz, 2H); ^{13}C NMR (100 MHz, DMSO-d_6) δ (ppm) 16.7, 117.9, 119.7, 123.8, 133.4, 133.5, 137.1, 149.8, 150.3, 172.1;MS (EI) m/z 169 (100%), 318 (M^+); HRMS Calcd. for $C_{14}H_{11}{}^{79}BrN_2O_2$: 318.0004, Found: 317.9996, $C_{14}H_{11}{}^{81}BrN_2O_2$: 319.9983, Found: 319.9999; Anal. Calcd. for $C_{14}H_{11}BrN_2O_2$: C 52.69, H 3.49, N 8.78, Found: C 52.81, H 3.43, N 8.73.

*4.1.18. (E)-5-(3-Trifluoromethyl-4-cyanophenyl)-2-hydroxycyclohepta-2,4,6-trienone (**1r**)*

Compound **1r** was prepared by the same method as described for the synthesis of **1a** using 4-amino-2-(trifluorometyl)benzonitrile (376 mg, 2.0 mmol) instead of aniline; 53 mg (8% yield); dark brown needles (AcOEt); mp 193–194 °C; ^{1}H NMR (400 MHz, DMSO-d_6) δ (ppm) 7.27 (d, J = 12.0 Hz, 2H), 8.11 (d, J = 11.6 Hz, 2H), 8.21 (d, J = 8.8 Hz, 1H), 8.25 (s, 1H), 8.35 (d, J = 8.1 Hz, 1H); ^{13}C NMR (100 MHz, DMSO-d_6) δ (ppm) 115.3, 119.3, 120.9, 123.6, 124.1, 126.3, 132.3, 134.2, 137.2, 148.6, 152.8, 173.7; MS (EI) m/z 319 (M^+, 100%); HRMS Calcd. for $C_{15}H_8F_3N_3O_2$: 319.0569, Found: 319.0573; Anal. Calcd. for $C_{15}H_8F_3N_3O_2$: C 56.43, H 2.53, N 13.17, Found: C 56.65, H 2.42, N 13.22.

*4.1.19. (E)-5-((3,5-Dimethylphenyl)diazenyl)-2-hydroxycyclohepta-2,4,6-trienone (**1s**)*

Compound **1s** was prepared by the same method as described for the synthesis of **1a** using 3,5-dimethylaniline (336 mg, 2.8 mmol) instead of aniline; 30 mg (5% yield); brown prisms (AcOEt); mp 162–164 °C; ^{1}H NMR (400 MHz, DMSO-d_6) δ (ppm) 2.37 (s, 6H), 7.20 (s, 1H), 7.37 (d, J = 12.0 Hz, 2H), 7.49 (s, 2H), 8.07 (d, J = 11.6 Hz, 2H); ^{13}C NMR (100 MHz, DMSO-d_6) δ (ppm) 20.7, 120.3, 123.8, 132.8, 133.0, 138.7, 149.7, 151.7, 171.8; MS (EI) m/z 105 (100%), 254 (M^+); HRMS Calcd. for $C_{15}H_{14}N_2O_2$: 254.1056, Found: 254.1045; Anal. Calcd. for $C_{15}H_{14}N_2O_2$: C 70.85, H 5.55, N 11.02, Found: C 70.96, H 5.63, N 10.99.

*4.1.20. (E)-5-((3,5-Bis(trifluoromethyl)phenyl)diazenyl)-2-hydroxycyclohepta-2,4,6-trienone (**1t**)*

Compound **1t** was prepared by the same method as described for the synthesis of 1a using 3,5-bis(trifluoromethyl)aniline (2.31 g, 10 mmol) instead of aniline; 2.25 g (62% yield); red/brown thin needles (AcOEt); mp 194–196 °C; ^{1}H NMR (400 MHz, DMSO-d_6) δ (ppm) 7.34 (d, J = 12.0 Hz, 2H), 8.18 (d, J = 12.4 Hz, 2H), 8.28 (s, 1H), 8.43 (s, 2H); ^{13}C NMR (100 MHz, DMSO-d_6) δ (ppm) 121.6, 122.7, 123.7, 124.3, 131.6, 133.9, 149.0, 152.1, 172.8; MS (EI) m/z 362 (M^+, 100%); HRMS Calcd. for $C_{15}H_8F_6N_2O_2$: 362.0490, Found: 362.0494; Anal. Calcd. for $C_{15}H_8F_6N_2O_2$: C 49.73, H 2.23, N 7.74, Found: C 49.57, H 2.14, N 7.65.

*4.1.21. (E)-5-((3,4,5-Trimethoxyphenyl)diazenyl)-2-hydroxycyclohepta-2,4,6-trienone (**1u**)*

Compound **1u** was prepared by the same method as described for the synthesis of **1a** using 3,4,5-trimethoxyaniline (370 mg, 2.0 mmol) instead of aniline; 215 mg (34% yield); purple needles (AcOEt); mp 156–160 °C; ^{1}H NMR (270 MHz, DMSO-d_6) δ (ppm) 3.75 (s, 3H), 3.88 (s, 6H), 7.25 (s, 2H), 7.36 (d, J = 12.2 Hz, 2H), 8.11 (d, J = 12.2 Hz, 2H); ^{13}C NMR (100 MHz, DMSO-d_6) δ (ppm) 56.0, 60.3, 100.4, 123.9, 132.8, 140.5, 147.5, 149.5, 153.4, 171.8; MS (EI) m/z 316 (M^+, 100%); HRMS Calcd. for $C_{16}H_{16}N_2O_5$: 316.1059, Found: 316.1062; Anal. Calcd. for $C_{16}H_{16}N_2O_5$: C 60.75, H 5.10, N 8.86, Found $C_{16}H_{16}N_2O_5$: C 60.47, H 5.04, N 8.72.

*4.1.22. (E)-5-((3,5-Bis(trifluoromethyl)phenyl)diazenyl)-2-methoxycyclohepta-2,4,6-trienone (**2**)*

A 2 M of solution of TMS diazomethane (4.5 mL, 9.0 mmol) was added dropwise to a solution of **1t** (1.10 g, 3.04 mmol) in 30 mL of THF and 20 mL of MeOH at 0 °C. The mixture was stirred for 1 h at room temperature, and subsequently quenched by the addition of 5 mL of acetic acid. The crude mixture was concentrated to afford 1.32 g (quantitative yield) of crude **2**, which was purified by recrystallization from AcOEt to afford 353 mg (31% yield) of red/brown thin needles; mp 187–189 °C; ^{1}H NMR (400 MHz, DMSO-d_6) δ (ppm) 4.09 (s, 3H), 6.98 (d, J = 10.8 Hz, 1H), 7.32 (d, J = 13.2 Hz, 1H), 7.99 (s, 1H), 8.02 (dd, J = 2.0 Hz, 10.8 Hz, 1H), 8.13 (dd, J = 2.0 Hz, 13.0 Hz, 1H), 8.34 (s, 2H); ^{13}C NMR (100 MHz, DMSO-d_6) δ (ppm) 56.4, 110.3, 121.6, 122.9, 124.0, 126.5, 132.8, 136.2, 138.1, 150.3, 152.3, 165.4, 180.1; MS (EI) m/z 376 (M^+, 100%); HRMS Calcd. for $C_{16}H_{10}F_6N_2O_2$: 376.0647, Found: 376.0655; Anal. Calcd. for $C_{16}H_{10}F_6N_2O_2 \cdot 0.1$ AcOEt: C 51.15, H 2.83, N 7.28, Found: C 51.39, H 2.79, N 7.00.

4.2. Biological assays

4.2.1. Xanthine-oxidase (XO)-inhibitory assay

Reaction mixtures containing 100 mM phosphate buffer (pH = 7.4), 0.01 U/mL of xanthine oxidase (Oriental Yeast), and the test compounds in DMSO at specific concentrations (100 μM – 10 nM) were incubated at 25 °C for 15 min. Allopurinol was used as a positive control. The reactions were started by addition of 150 μM of xanthine (Wako). After 8 min, the enzymatic reactions were stopped by addition of hydrochloric acid (1 M, 25 μM), and the production of uric acid was estimated based on the absorbance at 290 nm. IC_{50} values for each compound were calculated using the GraphPad Prism 4.0 software. Final concentrations of DMSO (0.5%) did not interfere with the enzyme activity.

4.2.2. Kinetic studies

Reaction mixtures containing 100 mM phosphate buffer (pH = 7.4), 0.01 U/mL of XO, and **1j** at 0.25 μM, 0.5 μM, or 1.0 μM were incubated at 25 °C for 15 min. The reactions were started by addition of xanthine solutions (22.5 μM, 30 μM, 45 μM, or 60 μM). After 5 min, the enzymatic reactions were stopped by addition of hydrochloric acid (1 M, 25 μM) and the production of uric acid was estimated based on the absorbance at 290 nm. Michaelis-Menten and Lineweaver-Burk plots were prepared in order to analyze the enzyme kinetics using the data obtained. V_{max} and K_m values of **1j** at each concentration were calculated

from the intersections of x- and y-axes in the Lineweaver-Burk plots.

4.3. Computational study

Three-dimensional (3D) structures of protein-ligand complexes were predicted using the Discovery Studio 4.5/CDOCKER software (BIOVIA) with default settings. The 3D structures of XO used in this study were retrieved from the RCSB Protein Data Bank (PDB ID: 1N5X). Missing hydrogen atoms in the crystal structure were computationally added and the center of the active site was defined as the center of the ligand in 1N5X. The conformation of **1j** was optimized using the CHARMm force field and docking simulation of **1j** with 1N5X (CDOCKER protocol). The docking pose with the highest CDOCKER INTERACTION ENERGY was selected for the discussion of twelve docking modes.

Acknowledgments

The work described in this paper was supported by a grant-in-aid from the Strategic Research Program for Private Universities (2015–2019) from the Japanese Ministry of Education, Culture, Sports, Sciences, and Technology (MEXT).

References and notes

1. Hille, R.; Hall, J.; Basu, P. The mononuclear molybdenum enzymes. *Chem. Rev.* **2014**, *114*, 3963–4038.
2. Nishino, T.; Okamoto, K. Mechanistic insights into xanthine oxidoreductase from development studies of candidate drugs to treat hyperuricemia and gout. *J. Biol. Inorg. Chem.* **2015**, *20*, 195–207.
3. Elion, G. B. The purine path to chemotherapy. *Science* **1989**, *244*, 41–47.
4. Hung, S. I.; Chung, W. H.; Liou, L. B.; Chu, C. C.; Lin, M.; Huang, H. P.; Lin, Y. L.; Lan J. L.; Yang, L. C.; Hong, H. S.; Chen M. J.; Lai, P. C.; Wu, M. S.; Chu, C. Y.; Wang, K. H.; Chen, C. H.; Fann, C. S.; Wu, J. Y.; Chen Y. T. HLA-B*5801 allele as a genetic marker for severe cutaneous adverse reactions caused by allopurinol. *Proc. Natl. Acad. Sci. USA* **2005**, *102*, 4134–4139.
5. Stamp, L. K.; Day, R. O.; Yun, J. Allopurinol hypersensitivity: investigating the cause and minimizing the risk. *Nat. Rev. Rheumatol*. **2016**, *12*, 235–242.
6. Hosoya, T.; Kimura, K.; Itoh, S.; Inaba, M.; Uchida, S.; Tomino, Y.; Makino, H.; Matsuo, S.; Yamamoto, T.; Ohno, I.; Shibagaki, Y.; Iimuro, S.; Imai, N.; Kuwabara, M.; Hayakawa, H. The effect of febuxostat to prevent a further reduction in renal function of patients with hyperuricemia who have never had gout and are complicated by chronic kidney disease stage 3: study protocol for a multicenter randomized controlled study. *Trials*, **2014**, *15*, 1–9.
7. Spector, T.; Johns, D. G. Stoichiometric inhibition of reduced xanthine oxidase by hydroxypyrazolo [3,4-d]pyrimidines. *J. Biol. Chem.* **1970**, *245*, 5079–5085.
8. Okamoto, K.; Eger, B. T.; Nishino, T.; Pai, E. F.; Nishino, T. Mechanism of inhibition of xanthine oxidoreductase by allopurinol: crystal structure of reduced bovine milk xanthine oxidoreductase bound with oxipurinol. *Nucleosides, Nucleotides Nucleic Acids* **2008**, *27*, 888–893.
9. Okamoto, K.; Eger, B. T.; Nishino, T.; Kondo, S.; Pai, E. F.; Nishino T. An extremely potent inhibitor of xanthine oxidoreductase. *J. Biol. Chem.* **2003**, *278*, 1848–1855.
10. Kikuchi, H.; Fujisaki, H.; Furuta, T.; Okamoto, K.; Leimkühler, S.; Nishino, T. Different inhibitory potency of febuxostat towards mammalian and bacterial xanthine oxidoreductases: insight from molecular dynamics. *Sci. Rep.* **2012**, *2*, 331 (1–8).
11. Šmelcerović, A.; Tomović, K.; Šmelcerović, Ž.; Petronijević, Ž.; Kocić, G.; Tomašić, T.; Jakopin, Ž.; Anderluh, M. *Eur. J. Med. Chem.* **2017**, *135*, 491–516.
12. Liu, N.; Song, W.; Schienebeck, C. M.; Zhang, M.; Tang, W. Synthesis of naturally occurring tropones and tropolones. *Tetrahedron* **2014**, *70*, 9281–9305.
13. Suzuki, H.; Ueda, T.; Juranek, I.; Yamamoto, S.; Katoh, T.; Node, M.; Suzuki, T. Hinokitiol, a selective inhibitor of the platelet-type isozyme of arachidonate 12-lipoxygenase. *Biochem. Biophys. Res. Commun.* **2000**, *275*, 885–889.
14. Morita, Y.; Matsumura, E.; Okabe, T.; Shibata, M.; Sugiura, M.; Ohe, T.; Tsujibo, H.; Ishida, N.; Inamori, Y. Biological activity of tropolone. *Biol. Pharm. Bull.* **2003**, *26*, 1487–1490.
15. Jacobsen, J. A.; Fullagar, J. L.; Miller, M. T.; Cohen, S. M. Identifying chelators for metalloprotein inhibitors using a fragment-based approach. *J. Med. Chem.* **2011**, *54*, 591–602.
16. Ononye, S. N.; VanHeyst, M. D.; Oblak, E. Z.; Zhou, W.; Ammar, M.; Anderson, A. C.; Wright, D. L. Tropolones as lead-like natural products: The development of potent and selective histone deacetylase inhibitors. *ACS Med. Chem. Lett.* **2013**, *4*, 757–761.
17. Ebisawa, M.; Ohta, K.; Kawachi, E.; Fukasawa, H.; Hashimoto, Y.; Kagechika, H. Novel retinoidal tropolone derivatives. Bioisosteric Relationship of tropolone ring with benzoic acid moiety in retinoid structure. *Chem. Pharm. Bull.* **2001**, *49*, 501–503.
18. Becica, J.; Jackson, A. B.; Dougherty, W. G.; Kassel, W. S.; West, N. M. Bis-tropolonate complexes of tungsten: scaffolds for selective side-on binding of nitriles, imines and ketones. *Dalton Trans.* **2014**, *43*, 8738–8748.
19. Dwivedi, A. D.; Binnani, C.; Tyagi, D.; Rawat, K. S.; Li, P.-Z.; Zhao, Y.; Mobin, S. M.; Pathak, B.; Singh, S. K. Troponate/aminotroponate ruthenium-arene complexes: synthesis, structure, and ligand-tuned mechanistic pathway for direct C-H bond arylation with aryl chlorides in water. *Inorg. Chem.* **2016**, *55*, 6739–6749.
20. Nomura, M.; Imamura, F.; Nga, N. B. T.; Fujita-Takayama, C.; Sugiyama, T.; Kajitani, M. Synthesis and electrochemistry of organometallic cobaltadithiaazulenes. *Inorg. Chem.* **2012**, *51*, 10695–10703.
21. Minns R. A. *Org. Synth.* **1977**, *57*, 117–121.
22. Deveau, A. M.; Macdonald, T. L. Practical synthesis of biaryl colchinoids containing 3',4'-catechol ether-based A-rings via Suzuki cross-coupling with ligandless palladium in water. *Tetrahedron Lett.* **2004**, *45*, 803–807.
23. Ishibuchi, S.; Morimoto, H.; Oe, T.; Ikebe, T.; Inoue, H.; Fukunari, A.; Kamezawa, M.; Yamada, I.; Naka, Y. Synthesis and structure-activity relationships of 1-phenylpyrazoles as xanthine oxidase inhibitors. *Bioorg. Med. Chem. Lett.* **2001**, *11*, 879–882.
24. Tang, H.-J.; Zhang, X.-W.; Yang, L.; Li, W.; Li, J.-H.; Wang, J.-X.; Chen, J. Synthesis and evaluation of xanthine oxidase inhibitory and antioxidant activities of 2-arylbenzo[b]furan derivatives based on salvianolic acid C. *Eur. J. Med. Chem.* **2016**, *124*, 637–648.
25. March's advanced organic chemistry: Reactions, mechanisms, and structure; Smith, M. B.; March, J., Eds., 5th ed.; *Wiley-Interscience*: New York, **2001**.
26. Wu, G.; Robertson, D. H.; Brooks, C. L. III; Vieth, M. Detailed analysis of grid-based molecular docking: A case study of CDOCKER—A CHARMm-based MD docking algorithm. *J. Comp. Chem.* **2003**, *24*, 1549–1562.